CERAMICS
INTERNATIONAL

Theoretical study of the molecular structure for zirconium complexes

M. Ángeles Díaz-Díez[a], Antonio Macías-García[a,*], Guadalupe Silvero[b],
Ruth Gordillo[b], Ricardo Caruso[c]

[a]Área de Ciencia de Materiales e Ingeniería Metalúrgica, Escuela de Ingenierías Industriales,
Universidad de Extremadura, Avda. Elvas s/n, 06071 Badajoz, Spain
[b]Departamento de Química Orgánica, Facultad de Ciencias, Universidad de Extremadura, Avda. Elvas s/n, 06071 Badajoz, Spain
[c]Laboratorio de Materiales Cerámicos, Facultad de Ciencias Exactas, Ingeniería y Agrimensura, Universidad Nacional de Rosario,
(IFIR-CONICET), Pellegrini 250, (2000) Rosario, Argentina. Member, CONICET, Argentina

Abstract

This work constitutes a study guided to the design of the molecular geometry of ZrO_2 gels aided by computer-based calculations (Density-Functional Theory). The electronic and spectroscopic properties of two zirconium complexes, $[Zr(OH)_6]^{2-}$ and $[Zr(OH)_5(OCH_2CH_2CH_3)]^{2-}$, are explored. Vibration frequencies and properties of nuclear magnetic resonance are theoretically studied.
© 2003 Elsevier Science Ltd and Techna S.r.l. All rights reserved.

Keywords: A. Sol–gel processes; A. Precursors; D. ZrO_2; Molecular structure; Computational study; DFT

1. Introduction

The sol–gel method is considered a very important route to produce homogeneous materials with particular physical and chemical properties [1]. In particular, the preparation of ZrO_2-based ceramic by the sol–gel process is an area of interest for the technological applications of these materials [2,3].

Sol-gel chemistry is based on inorganic polymerization reactions. Sol-gel processing involves the use of molecular precursors, mainly alkoxides as starting materials. In general, the alkoxides are dissolved in alcohol and hydrolyzed with H_2O in presence of an acid or basic catalyst [4]. A macromolecular oxide network is then obtained through hydrolysis and condensation reactions. These reactions play a significant role in the final gel molecular structure. The kind and amount of catalyst used, the amount of water and the nature of solvent have an influence on the hydrolysis to condensation ratio and thereby determine the properties of the resulting sol–gel product. The properties of the obtained materials will depend on the molecular structure of the precursors gels [5,6].

Computer-based calculations are now used in practically all branches of chemistry. For several decades they have been developed and refined so that they now allow analyzing the structure and properties of matter in detail. Conventional calculation of the properties of molecules is based on a description of the motion of individual electrons. For this reason, such methods are mathematically very complicated. Walter Kohn showed that it is not necessary to consider the motion of each individual electron: it suffices to know the average number of electrons located at any one point in space. This has led to a computationally simpler method, the Density-Functional Theory (DFT) [7]. The simplicity of the method makes it possible to study very large molecules.

With these premises our research group decided to explore electronic and spectroscopic properties of two model zirconium complexes: $[Zr(OH)_6]^{2-}$ (**1**) and $[Zr(OH)_5(OCH_2CH_2CH_3)]^{2-}$ (**2**). The scope of this work was to determine the theoretical molecular structure, the IR spectra and the NMR shielding tensor of the studied complexes.

---

* Corresponding author.
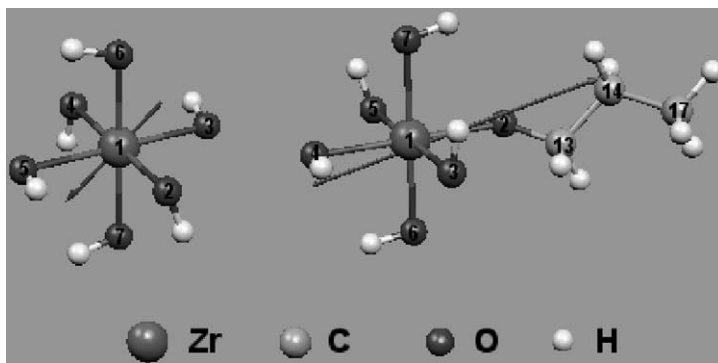*E-mail address:* amacias@materiales.unex.es (A. Macías-García).

Fig. 1. Optimized structures and dipolar moment vectors for models **1** and **2**.

Table 1
Interatomic distances and angles of model **1**

Interatomic distances (Å)		Interatomic angles (degrees)			
Zr(1)–O(2)	2.158	O(2)–Zr(1)–O(3)	89.703	O(5)–Zr(1)–O(6)	90.294
Zr(1)–O(3)	2.131	O(2)–Zr(1)–O(4)	180.000	O(5)–Zr(1)–O(7)	89.712
Zr(1)–O(4)	2.162	O(2)–Zr(1)–O(5)	89.764	Zr(1)–O(2)–H(13)	100.923
Zr(1)–O(5)	2.187	O(2)–Zr(1)–O(6)	90.000	Zr(1)–O(3)–H(12)	99.315
Zr(1)–O(6)	2.134	O(2)–Zr(1)–O(7)	89.790	Zr(1)–O(4)–H(11)	101.352
Zr(1)–O(7)	2.188	O(3)–Zr(1)–O(4)	90.534	Zr(1)–O(5)–H(10)	98.827
O(2)–H(13)	0.971	O(3)–Zr(1)–O(5)	179.451	Zr(1)–O(6)–H(8)	101.560
O(3)–H(12)	0.971	O(3)–Zr(1)-O(6)	89.731	Zr(1)–O(7)–H(9)	100.932
O(4)–H(11)	0.972	O(3)–Zr(1)–O(7)	90.261	Zr(1)–O(2)–H(13)	100.923
O(5)–H(10)	0.971	O(4)–Zr(1)–O(5)	89.999	Zr(1)–O(3)–H(12)	99.315
O(6)–H(8)	0.972	O(4)–Zr(1)–O(6)	90.000	Zr(1)–O(4)–H(11)	101.352
O(7)–H(9)	0.972	O(4)–Zr(1)–O(7)	90.207	Zr(1)–O(5)–H(10)	98.827
				Zr(1)–O(6)–H(8)	101.560

Table 2
Interatomic distances and angles of model **2**

Interatomic distances (Å)		Interatomic angles (degrees)			
Zr(1)–O(2)	2.201	O(2)–Zr(1)–O(3)	89.701	Zr(1)–O(4)–H(11)	101.731
Zr(1)–O(3)	2.119	O(2)–Zr(1)–O(4)	180.000	Zr(1)–O(5)–H(10)	102.476
Zr(1)–O(4)	2.125	O(2)–Zr(1)–O(5)	89.766	Zr(1)–O(6)–H(8)	102.411
Zr(1)–O(5)	2.182	O(2)–Zr(1)–O(6)	90.000	Zr(1)–O(7)–H(9)	102.873
Zr(1)–O(6)	2.128	O(2)–Zr(1)–O(7)	89.790	O(2)–C(13)–C(14)	112.235
Zr(1)–O(7)	2.177	O(3)–Zr(1)–O(4)	90.541	O(2)–C(13)–H(15)	112.728
O(2)–C(13)	1.365	O(3)–Zr(1)–O(5)	179.451	O(2)–C(13)–H(16)	112.532
O(3)–H(12)	0.970	O(3)–Zr(1)–O(6)	89.731	C(14)–C(13)–H(15)	107.398
O(4)–H(11)	0.971	O(3)–Zr(1)–O(7)	90.261	C(14)–C(13)–H(16)	105.896
O(5)–H(10)	0.971	O(4)–Zr(1)–O(5)	89.993	H(15)–C(13)–H(16)	105.546
O(6)–H(8)	0.971	O(4)–Zr(1)–O(6)	90.002	C(13)–C(14)–C(17)	113.901
O(7)–H(9)	0.972	O(4)–Zr(1)–O(7)	90.208	C(13)–C(14)–H(18)	108.209
C(13)–C(14)	1.551	O(5)–Zr(1)–O(6)	90.298	C(13)–C(14)–H(119)	108.026
C(13)–H(15)	1.112	O(5)–Zr(1)–O(7)	89.708	C(17)–C(14)–H(18)	110.133
C(13)–H(16)	1.123	O(6)–Zr(1)–O(7)	180.000	C(17)–C(14)–H(19)	109.947
C(14)–C(17)	1.534	Zr(1)–O(2)–H(13)	129.148	H(18)–C(14)–H(19)	106.321
C(14)–H(18)	1.100	O(2)–Zr(1)–O(3)	89.701	C(14)–C(17)–H(20)	112.960
C(14)–H(19)	1.099	O(2)–Zr(1)–O(4)	180.000	C(14)–C(17)–H(21)	110.769
C(17)–H(20)	1.101	O(2)–Zr(1)–O(5)	89.766	C(14)–C(17)–H(22)	110.939
C(17)–H(21)	1.100	O(2)–Zr(1)–O(6)	90.000	H(20)–C(17)–H(21)	107.543
C(17)–H(22)	1.100	O(2)–Zr(1)–O(7)	89.790	H(20)–C(17)–H(22)	107.479
		Zr(1)–O(3)–H(12)	100.100	H(21)–C(17)–H(22)	106.881

Table 3
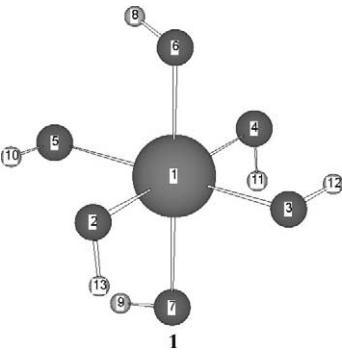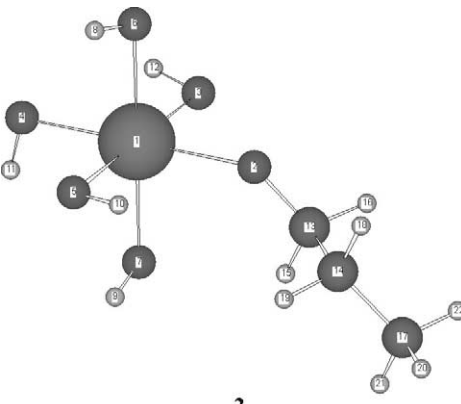Bands and vibration mode in theoretical IR spectra of models **1** and **2**

Compound	cm^{-1}	Vibration mode
1	384	Symmetric Zr–O
	420	Asymmetric Zr–O
	430	Out-of-plane OH
	435	
	501	
	512	
	619	In-plane OH
	649	
	651	
	662	
	671	
	673	
2	409	Symmetric and asymmetric Zr–O
	411	
	475	
	382	Out-of-plane OH
	431	
	486	
	531	
	529	In-plane OH
	644	
	648	
	664	
	765	
	1205	Symmetric C–O

Table 4
Predicted chemical shifts (δ ppm) in model **1**

H8	H9	H10	H11	H12	H13
1.68	−0.47	0.19	0.68	2.14	0.83

From the results of this work and in a future stage, the authors aim to obtain ZrO_2 gels with different molecular structure from sol–gel solutions prepared by different synthetic routes. Afterwards we will carry out IR and NMR analysis to obtain the experimental spectra of these samples. Finished this stage, the coincidence of these experimental spectra with the theoretical obtained in this work will be examined. This will allow us to investigate the existent correlation between the structure and microstructure of the prepared samples with the results of theoretical calculations carried out in this work.
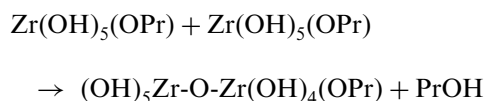
2. Experimental

Calculations were performed using the GAUSSIAN94 series of programs [8]. The Becke3LYP hybrid functional, consisting of the non local exchange functional of Becke's three-parameter set, and the non local correlation function of Lee et al. [7], were used together with the 6-31G(d) basis set [9] for C, H, O and Si nuclei, and the LANL1MB basis set [10] for the Zr nucleus. Both geometries were fully optimized and all the calculated frequencies animated using MOLDEN [11] in order to assign every band of the IR spectrum to a vibration mode of the molecule.
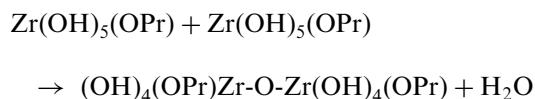
3. Results and discussions

Fig. 1 shows optimized structures for models **1** and **2**, which correspond with hexacoordinated zirconium

Table 5
Predicted chemical shifts (δ ppm) in model **2**

H8	H9	H10	H11	H12	H15	H16	H18	H19	H20	H21	H22	C13	C14	C17
1.24	1.17	−0.13	−0.09	2.39	5.29	4.12	0.95	1.03	0.05	0.57	0.41	67.1	30.2	7.39

complexes in the form of tetragonal bi-pyramid. In the case of **1**, a partial charge of $+1.34$ a.u. was observed on zirconium atom whereas the negative charge is almost equally distributed on oxygen atoms. For this molecule, a theoretical dipole moment of 2.66 debyes was found. Model **2** presented a dipole moment of 6.50 debyes and, again, a partial positive charge of 1.38 a.u. is localized on the metallic nucleus. Oxygen 2 support a partial negative charge of 0.70 a.u. and the remaining oxygen atoms support a partial negative charge of about 0.50 a.u.

The higher dipole moment in model **2**, and in consequence, the increased polarity found is due to the presence of the propoxide group. The partial negative charge supported by oxygen labeled as 2 in that model, would favor possible protonation and further hydrolysis reactions on this nucleus. For molecules that are in solution, condensation reactions could also occur between two metal-alkoxide molecules. For acid-promoted reactions, the most probable process can be written as follows:

$$Zr(OH)_5(OPr) + Zr(OH)_5(OPr)$$

$$\rightarrow (OH)_5Zr\text{-}O\text{-}Zr(OH)_4(OPr) + PrOH$$

but not:

$$Zr(OH)_5(OPr) + Zr(OH)_5(OPr)$$

$$\rightarrow (OH)_4(OPr)Zr\text{-}O\text{-}Zr(OH)_4(OPr) + H_2O$$

These condensation reactions will lead to long chains of polymers with tendency to be linked in primary form. In contrast, for the model **1** the condensation reactions among molecules can occur without distinction between any groups –OH. This condensation mechanism will lead to molecules clusters with form of branch and more complex.

The calculated values for the interatomic distances and angles of the two explored zirconium complexes are listed in Tables 1 and 2.

As it can be observed, the structural parameters found for both complexes show the expected octahedric geometry, only distorted by the propoxide group in model **2**. This alkylic moiety does not affect the value of the distance between Zr and O atoms, found to have an average value of 2.15 Å.

Our computational study allowed obtaining the theoretical IR spectra of models **1** and **2**. Table 3 lists the most significant bands found in every case, and the corresponding vibration mode.

The most important difference observed in the theoretical IR spectra of both models was the significant gap between 700 and 3500 cm^{-1}, found in complex **1** infrared spectrum, and attributed to the lacking alkylic chain

existing in model **2**. The rest of peaks showed in both spectra were due to the expected *symmetric*, *asymmetric*, *out-of-plane* and *in-plane* possible vibrations for the different Zr–O, O–H and C–O bonds (Table 3).

NMR shielding tensor is another property that can be computed in the context of a single point energy calculation [12]. Shielding constants reported in experimental studies are usually shifts relative to a standard compound, often tetramethylsilane (TMS). In order to compare predicted values to experimental results, absolute shielding value for TMS is computed for fully optimized TMS molecule. To obtain the predicted shift for every atom it is necessary to subtract its absolute value from that of the reference molecule. Tables 4 and 5 show predicted chemical shifts (δ) in ppm for carbon and hydrogen nuclei in models **1** and **2**.

According to chemical shifts listed in Table 4, protons labeled as H8 and H12 in model **1** are the most deshielded ones, appearing downfield (high δ values). This fact is due to the higher electronic density on this area, as it was previously showed with dipole moment vectors in Fig. 1. On the other hand, protons H9 and H10 appear upfield, (low δ values). In the case of model **2** (Table 5), H15 and H16, attached to C13, directly bonded to O2, are the most deshielded ones. In same way, C13 is the most deshielded too.

4. Conclusions

Through the computational study carried out in this work we calculate the partial charge distribution, dipole moment and optimized structures of two zirconium complexes: $[Zr(OH)_6]^{2-}$ and $[Zr(OH)_5(OCH_2CH_2CH_3)]^{2-}$, theoretically. Also, our computational study allowed obtaining the theoretical IR spectra and the NMR shielding tensor of both complexes. From this information, it would be possible to make some predictions about the hydrolysis and condensation reactions of these complexes during the sol–gel process.

References

[1] C.J. Brinker, G.W. Scherer, Sol–Gel Science: The Physics and Chemistry of Sol–Gel Processing, Academic Press, San Diego, 1990.

[2] M. Atik, M.A. Aegerter, in: Proc. Sixth International Workshop on Glasses and Ceramics from Gels, Seville 1991, J. Non-Cryst. Solids, 1992, pp. 147–148, 813–819.

[3] B.J.J. Zelinski, D.R. Uhlmann, Gel technology in ceramics, J. Phys. Chem. Solids 45 (10) (1984) 1069.

[4] J. Livaje, M. Henry, C. Sanchez, Prog. Solid State Chem. 18 (1988) 259.

[5] B.E. Yoldas, J. Non-Cryst. Solids 63 (1984) 145.

[6] B.E. Yoldas, Material Research Society Symposium Proceeding, Elsevier Science, New York, 1984.

[7] (a) W. Kohn, L.J. Sham, Phys. Rev. 140 (1965) A1133;

(b) J.C. Slater, Quantum Theory of Molecular and Solids, McGraw-Hill, New York, 1974;

(c) S.H. Vosko, L. Wilk, M. Nusair, Canadian J. Phys. 58 (1980) 1200;

(d) C. Lee, W. Yang, R.G. Parr, Phys. Rev. B 37 (1988) 785–789;

(e) A.D. Becke, Phys. Rev. A 38 (1988) 3098;

(f) A.D. Becke, J. Chem. Phys. 98 (1993) 1372;

(g) R.G. Parr, Yang, Density-Functional Theory of Atoms and Molecules, Oxford University Press, Oxford, 1989.

[8] M.J. Frisch, G.W. Trucks, H.B. Schlegel, P.M.W. Gill, B.G. Johnson, M.A. Robb, J.R. Cheeseman, T.A. Keith, G.A. Petersson, J.A. Montgomery, K. Raghavachari, M.A. Al-Laham, V.G. Zakrzewski, J.V. Ortiz, J.B. Foresman, J. Cioslowski, B.B. Stefanov, A. Nanayakkara, M. Challacombe, C.Y. Peng, P.Y. Ayala, W. Chen, M.W. Wong, J.L. Andres, E.S. Replogle, R. Gomperts, R.L. Martin, D.J. Fox, J.S. Binkley, D.J. Defrees, J. Baker, J.P. Stewart, M. Head-Gordon, C. González, J.A. Pople, Gaussian, Inc., Pittsburgh PA, 1995.

[9] W.J. Hehre, L. Radom, P.v.R. Schleyer, J.A. Pople, Ab Initio Molecular Orbital Theory, Wiley, New York, 1986.

[10] (a) P.J. Hay, W.R. Wadt, J. Chem. Phys. 82 (1985) 270;

(b) P.J. Hay, W.R. Wadt, J. Chem. Phys. 8 (1985) 284;

(c) P.J. Hay, W.R. Wadt, J. Chem. Phys. 82 (1985) 299.

[11] G. Schaftenaar, J.H. Noordik, J. Comput.-Aided Mol. Des. 14 (2000) 123–134.

[12] J.R. Cheeseman, G.W. Trucks, T.A. Keith, M.J. Frisch, J. Chem. Phys. 104 (1996) 5497.